

Short communication

Effect of metal-substitution on the redox behaviors of mono-transition metal-substituted Wells–Dawson tungstoarsenates



Jung Ho Choi^a, Tae Hun Kang^a, Yongju Bang^a, Jong Kwon Lee^a, Jae Chun Song^b, In Kyu Song^{a,*}

^a School of Chemical and Biological Engineering, Institute of Chemical Processes, Seoul National University, 1 Gwanak-ro, Gwanak-Gu, Seoul 151-744, South Korea

^b Hanwha Chemical Corp., Daejeon 305-804, South Korea

ARTICLE INFO

Article history:

Received 5 December 2014

Received in revised form 25 February 2015

Accepted 26 February 2015

Available online 27 February 2015

Keywords:

Redox behavior

Tungstoarsenate

Cyclic voltammetry

UV–visible spectroscopy

Oxidative dehydrogenation of benzylamine

ABSTRACT

Mono-transition metal (Mo, V, and Nb)-substituted Wells–Dawson tungstoarsenates were investigated to elucidate the effect of metal-substitution on their redox behaviors. In the electrochemical analysis, an additional redox transition was observed for molybdenum- and vanadium-substituted tungstoarsenates, while a negatively shifted redox transition was observed for niobium-substituted tungstoarsenate. First electron reduction potential of the catalysts showed the consistent trend with UV–visible absorption edge energy of the catalysts. Oxidative dehydrogenation of benzylamine to dibenzylimine was carried out as a model reaction to probe oxidation catalysis. Yield for dibenzylimine increased with increasing first electron reduction potential and with decreasing UV–visible absorption edge energy.

© 2015 Elsevier B.V. All rights reserved.

1. Introduction

Heteropolyacids (HPAs) are polymeric metal–oxygen clusters that exhibit various physicochemical properties. HPAs are structurally well-defined than any other metal oxides and their physicochemical properties can be easily tuned by changing the constituent elements. This means that the design of HPAs is possible at molecular level to meet the need for specific catalytic applications.

HPAs are strong oxidizing agents or excellent redox catalysts because the addenda atoms in heteropolyanion frameworks are in their highest oxidation states. Thus, several structural classes of HPAs have been investigated as catalysts in the oxidation reactions and photocatalytic redox reactions [1–3]. Previous researches [4,5] on the oxidative dehydrogenation of alcohols over HPAs have suggested that the redox transition of HPAs occurs during the catalysis and the rate-determining step involves the reduction of HPAs by hydrogen and electron from the substrate. It is obvious that systematic researches on the redox nature of HPAs should be preferentially conducted before the catalytic applications. However, much progress has not been made on the redox nature of Wells–Dawson HPAs due to the structural diversity of mixed-addenda HPAs [6].

In this work, mono-transition metal (Mo, V, and Nb)-substituted Wells–Dawson tungstoarsenates were prepared to elucidate the effect of transition metal-substitution on their redox behaviors. Redox behaviors of the catalysts were examined by electrochemical analysis. UV–

visible spectroscopy measurement was also conducted as a simple diagnostic for electronic structure. Gas-phase oxidative dehydrogenation of benzylamine was carried out to track the oxidation catalysis of mono-transition metal-substituted Wells–Dawson tungstoarsenates.

2. Experimental

2.1. Preparation of catalyst

α -K₆As₂W₁₈O₆₂, α ₂-K₆As₂W₁₇Mo₁O₆₂, and α ₂-K₇As₂W₁₇V₁O₆₂ were prepared as described in the previous literature [7]. α ₂-K₇As₂W₁₇Nb₁O₆₂ was prepared by direct incorporation of niobium into mono-lacunary tungstoarsenate (α ₂-K₁₀As₂W₁₇O₆₁). For this, 0.4 g of oxalic acid (Sigma-Aldrich) was dissolved in 30 ml of deionized water. After complete dissolution, 0.110 g of niobium chloride (Sigma-Aldrich) was added to the solution. 1.70 g of mono-lacunary tungstoarsenate, which was prepared as described in the previous work [7], was separately dissolved in 20 ml of deionized water. These two solutions were then mixed. The mixed solution was treated with hydrochloric acid (Samchun Chem.) until the pH of the solution becomes ca. 1.0 and it was refluxed for 4 h. The resulting transparent solution was cooled to room temperature. The solution was added to 300 ml of methanol (Sigma-Aldrich) and the resultant was placed at 4 °C overnight. After a few days, white precipitate was collected and dried under room temperature to obtain α ₂-K₇As₂W₁₇Nb₁O₆₂.

Formation of Wells–Dawson heteropolyanion framework was confirmed by diffuse reflectance infrared Fourier transform (DRIFT) spectroscopy using a Nicolet 6700 (Nicolet) spectrometer. Chemical

* Corresponding author.

E-mail address: inksong@snu.ac.kr (I.K. Song).

compositions of the catalysts were analyzed by inductively coupled plasma-atomic emission spectroscopy (ICP-AES) analysis using an ICPS-1000IV (Shimadzu) instrumentation. In this work, mono-transition metal-substituted tungstoarsenates were denoted as $As_2W_{17}M_1$ ($M = W, Mo, V, \text{ and } Nb$).

2.2. Characterization

Electrochemical analysis was conducted to examine the electrochemical redox behaviors of mono-transition metal-substituted tungstoarsenates. Cyclic voltammograms were acquired using a conventional three-electrode system (Autolab 302N, Eco Chemie). Glassy carbon with a diameter of 3.0 mm, platinum rod, and saturated calomel electrode (KCl saturated) were used as a working electrode, a counter electrode, and a reference electrode, respectively. Each tungstoarsenate was dissolved in 0.5 M sodium sulfate electrolyte to prepare the sample solution (1 mM). The sample solution was pretreated with He flow prior to electrochemical measurements. Cyclic voltammograms were obtained at a scan rate of 25, 50, 100, 150, and 200 mV/s.

UV-visible spectroscopy measurement was performed as a simple diagnostic for electronic structure of mono-transition metal-substituted tungstoarsenates. UV-visible spectra were acquired using a Lambda-35 (Perkin-Elmer) spectrometer. The sample solution (1 mM) was prepared by dissolving each tungstoarsenate in deionized water to minimize the peripheral effect of coordinated water. Kubelka–Munk function ($F(R_{\infty})$) was employed to convert reflectance spectrum into equivalent absorption spectrum using $BaSO_4$ as a white standard [8]. Absorption edge energy was directly obtained from Tauc plot.

2.3. Catalytic test

Gas-phase oxidative dehydrogenation of benzylamine was carried out over mono-transition metal-substituted tungstoarsenates. 0.4 g of each catalyst was charged into the tubular quartz reactor and it was pretreated with a mixed stream of nitrogen (30 ml/min) and oxygen (10 ml/min) at 300 °C for 1 h. Benzylamine (7.2 mmol/h) was sufficiently vaporized by passing through the preheating zone and it was continuously fed into the reactor together with a mixed stream of nitrogen and oxygen. Catalytic reaction was carried out at 300 °C for 5 h. Reaction products were periodically sampled and were analyzed using a gas chromatograph (YL6100 GC, Younglin) equipped with a flame ionization detector. DB-5 (Agilent, 60 m \times 0.32 mm) capillary column was used for products separation. Conversion of benzylamine and yield for each product were calculated on the basis of carbon balance.

3. Results and discussion

3.1. Formation of heteropolyanion framework

Fig. 1 shows the DRIFT spectra of mono-transition metal-substituted tungstoarsenates. Several characteristic bands attributed to asymmetric vibrations of $M(\text{metal})=O_t$ (terminal oxygen), As–O, and M–O–M bonds were observed in the range of 1000–700 cm^{-1} , in good agreement with the results of previous literature [7]. For all catalysts, As–O bands appeared as a weak shoulder due to the intense and broad M–O–M bands. All the mono-transition metal-substituted tungstoarsenates exhibited slightly shifted bands compared to non-substituted one ($As_2W_{17}W_1$). Chemical compositions of arsenic, tungsten, and substituted-transition metal in the catalysts determined by ICP-AES analyses were in good agreement with the designed values (not shown here), supporting the successful formation of mono-transition metal-substituted tungstoarsenates. In this work, mono-transition metal-substituted tungstoarsenates were prepared by direct incorporation of transition metal into mono-lacunary tungstoarsenate ($\alpha_2\text{-K}_{10}As_2W_{17}O_{61}^{10-}$), which was derived from $\alpha\text{-K}_6As_2W_{18}O_{62}$

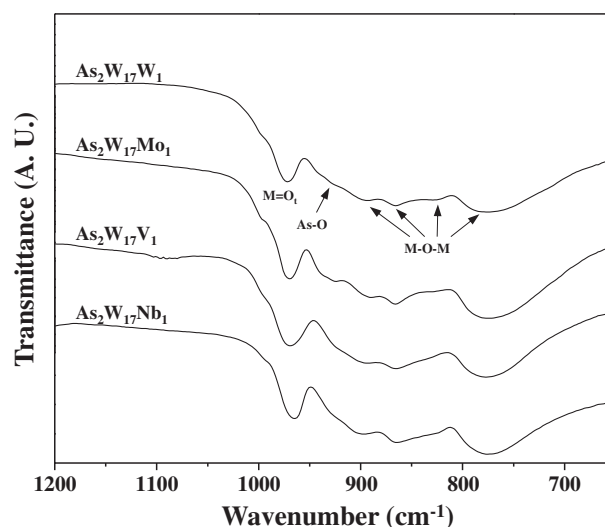


Fig. 1. DRIFT spectra of mono-transition metal-substituted tungstoarsenates.

via selective removal of WO_6 unit of cap site. Thus, transition metal could be selectively incorporated in the cap site of Wells–Dawson tungstoarsenate framework, providing the uniform structure to examine the effect of transition metal-substitution (in the cap site) on the redox behavior.

3.2. Cyclic voltammetry

Electrochemical analysis was conducted to examine the electrochemical redox behaviors of mono-transition metal-substituted tungstoarsenates. Fig. 2 shows the cyclic voltammograms of mono-transition metal-substituted tungstoarsenates obtained at a scan rate of 50 mV/s. All the catalysts exhibited reversible and stepwise redox transitions. Overall shapes of cyclic voltammograms were nearly unchanged even after several cycles of measurements, indicating that the catalysts were hydrolytically stable during the electrochemical measurements. Each peak current monotonically increased against the square root of scan rate, indicating that redox transitions shown in Fig. 2 were the diffusion-controlled reversible process that could be expressed by Randles–Sevcik equation [9].

$As_2W_{17}W_1$ exhibited four stepwise tungsten-centered redox couples. However, significantly different redox transitions were observed for mono-transition metal-substituted tungstoarsenates. For molybdenum- and vanadium-substituted tungstoarsenates, they exhibited an additional molybdenum- or vanadium-centered redox couple at higher potential region [10,11]. This indicates that molybdenum and vanadium centers in the tungstoarsenate frameworks are electrochemically more accessible and easier to be reduced than tungsten center. However, niobium-substituted tungstoarsenate did not exhibit any additional redox couple but showed a negatively-shifted redox couple compared to non-substituted one ($As_2W_{17}W_1$). In this work, first electron reduction potential was taken as a representative parameter for reducibility [12]. First electron reduction potential increased in the order of $As_2W_{17}Nb_1$ (-0.162 V) $<$ $As_2W_{17}W_1$ ($+0.049$ V) $<$ $As_2W_{17}Mo_1$ ($+0.243$ V) $<$ $As_2W_{17}V_1$ ($+0.378$ V), indicating that vanadium center was more effective to enhance the reducibility of tungstoarsenate framework than the other metal centers.

3.3. UV-visible spectroscopy

Previous research [13] has suggested that energy state and composition of the lowest unoccupied orbital (LUMO) play important roles in determining the redox behaviors of heteropolyanions. It is obvious

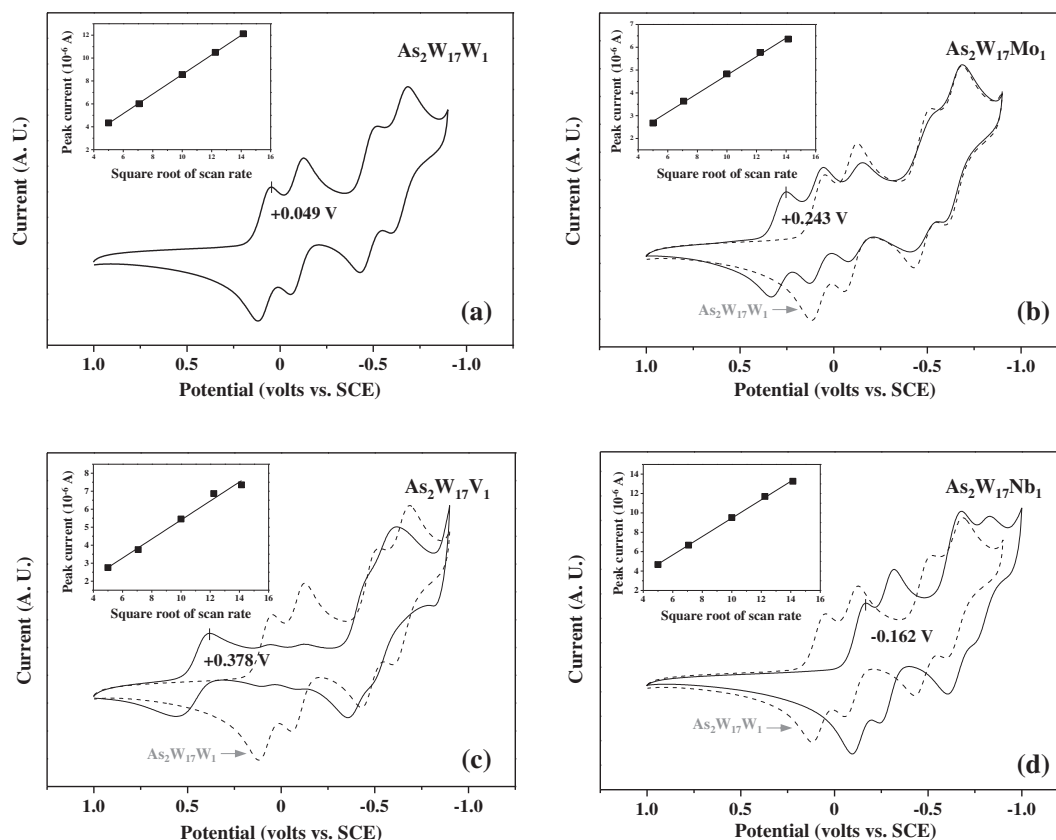


Fig. 2. Cyclic voltammograms of mono-transition metal-substituted tungstoarsenates obtained at a scan rate of 50 mV/s (each inset figure shows the peak current plotted as a function of square root of scan rate (for the first electron reduction)).

that energy state of the LUMO strongly depends on the nature of substituted-metal, because d-orbitals on the metal centers largely contribute to the LUMO of heteropolyanion. On the other hand, energy state of the highest occupied molecular orbital (HOMO) is little perturbed by metal-substitution, because the HOMO of heteropolyanion mostly comprises 2p-orbitals on the framework oxygens.

UV–visible spectroscopy measurement was performed as a simple diagnostic for electronic structure of mono-transition metal-substituted tungstoarsenates. Fig. 3(a) shows the Tauc plots of mono-transition metal-substituted tungstoarsenates for indirect-allowed

transition [14]. It is interesting to note that absorption edge energy, which corresponded to the energy gap between the HOMO and the LUMO, decreased in the order of $\text{As}_2\text{W}_{17}\text{Nb}_1$ (3.01 eV) > $\text{As}_2\text{W}_{17}\text{W}_1$ (2.97 eV) > $\text{As}_2\text{W}_{17}\text{Mo}_1$ (2.90 eV) > $\text{As}_2\text{W}_{17}\text{V}_1$ (2.36 eV). This indicates that vanadium center is the most effective to stabilize the energy level of the LUMO. Such stabilization effect by vanadium center has also been reported in the previous density functional theory (DFT) calculations [15]. It has been successfully demonstrated that the energy of tungsten center at cap sites is effectively stabilized by vanadium-substitution and the added electrons are preferentially delocalized over three vanadium centers in the reduced species. In this work, the

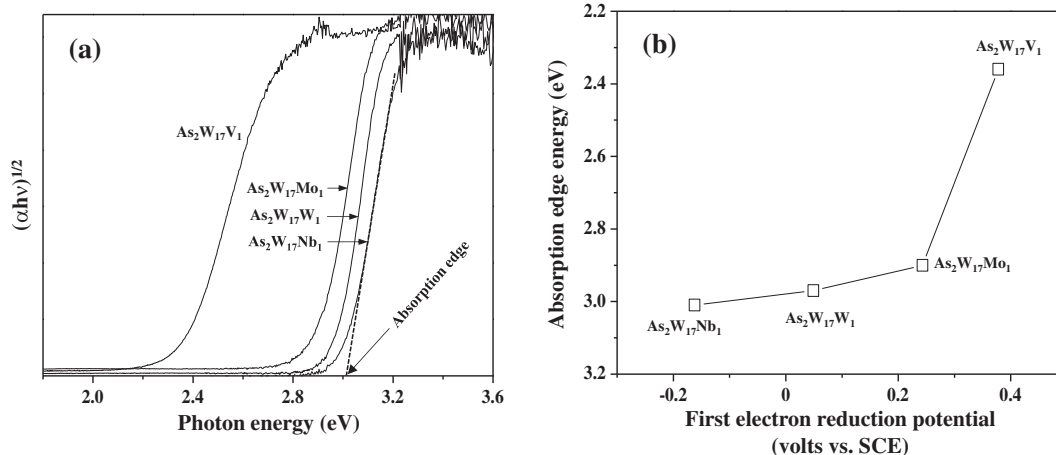


Fig. 3. (a) Tauc plots of mono-transition metal-substituted tungstoarsenates for indirect-allowed transition and (b) a correlation between first electron reduction potential and absorption edge energy.

effect of vanadium- or molybdenum-substitution on the energy state of the LUMO may be understood in the similar manner. The niobium center, which exhibits greater predisposition than vanadium or molybdenum center to lose its electrons (hard to be reduced), does not stabilize the energy level of the LUMO [15]. This trend was also consistently observed in a series of tri-transition metal (Mo, V, and Nb)-substituted Keggin tungstosilicates [13], indicating that metal-substitution showed the analogous effect on the redox behavior of heteropolyanion even in the different structures.

Fig. 3(b) shows the correlation between first electron reduction potential and absorption edge energy. Reduction potential increased with decreasing absorption edge energy. Although the effect of metal-substitution on the electronic structure is much complicated due to the presence of oxygen contribution to the LUMO, the correlation clearly shows that energy state of the LUMO depends on the nature of substituted metal. It also suggests that absorption edge energy can be utilized as an alternative parameter to estimate energy level of the LUMO and reduction potential of heteropolyanions in the series of mono-transition metal-substituted Wells–Dawson tungstoarsenates.

3.4. Gas-phase oxidative dehydrogenation of benzylamine

Gas-phase oxidative dehydrogenation of benzylamine was carried out over mono-transition metal-substituted tungstoarsenates. Fig. 4

shows the reaction pathway in the oxidative dehydrogenation of benzylamine over HPAs [16]. Dibenzylimine, benzonitrile, and benzaldehyde can be formed from the dehydrogenated intermediate (phenylmethanimine). Unstable phenylmethanimine reacts with another molecule of benzylamine to form aminal and then releases ammonia to form dibenzylimine. Benzonitrile can be formed by further oxidative dehydrogenation of phenylmethanimine. Benzaldehyde can be produced by hydrolysis of phenylmethanimine.

In this work, dibenzylimine was mainly formed over the catalysts. Trace amounts of benzonitrile and benzaldehyde were also detected during the reaction. It is noteworthy that none of them was detected without oxygen, supporting that dibenzylimine, benzonitrile, and benzaldehyde were formed via oxidative dehydrogenation reaction. It was also found that benzylamine readily reacted with benzaldehyde to form dibenzylimine even at room temperature, indicating that as-produced benzaldehyde could react with benzylamine to form dibenzylimine. Fig. 5(a) shows the catalytic performance of $As_2W_{17}W_1$ during a 5 h-reaction. Fig. 5(b) shows the conversion of benzylamine and product yield after a 5 h-reaction. All the catalysts exhibited a stable catalytic performance during a 5 h-reaction. Yield for dibenzylimine increased in the order of $As_2W_{17}Nb_1 < As_2W_{17}W_1 < As_2W_{17}Mo_1 < As_2W_{17}V_1$.

Fig. 6 shows the DRIFT spectra of fresh and used $As_2W_{17}W_1$ catalysts. Although slight changes in band position and signal intensity were

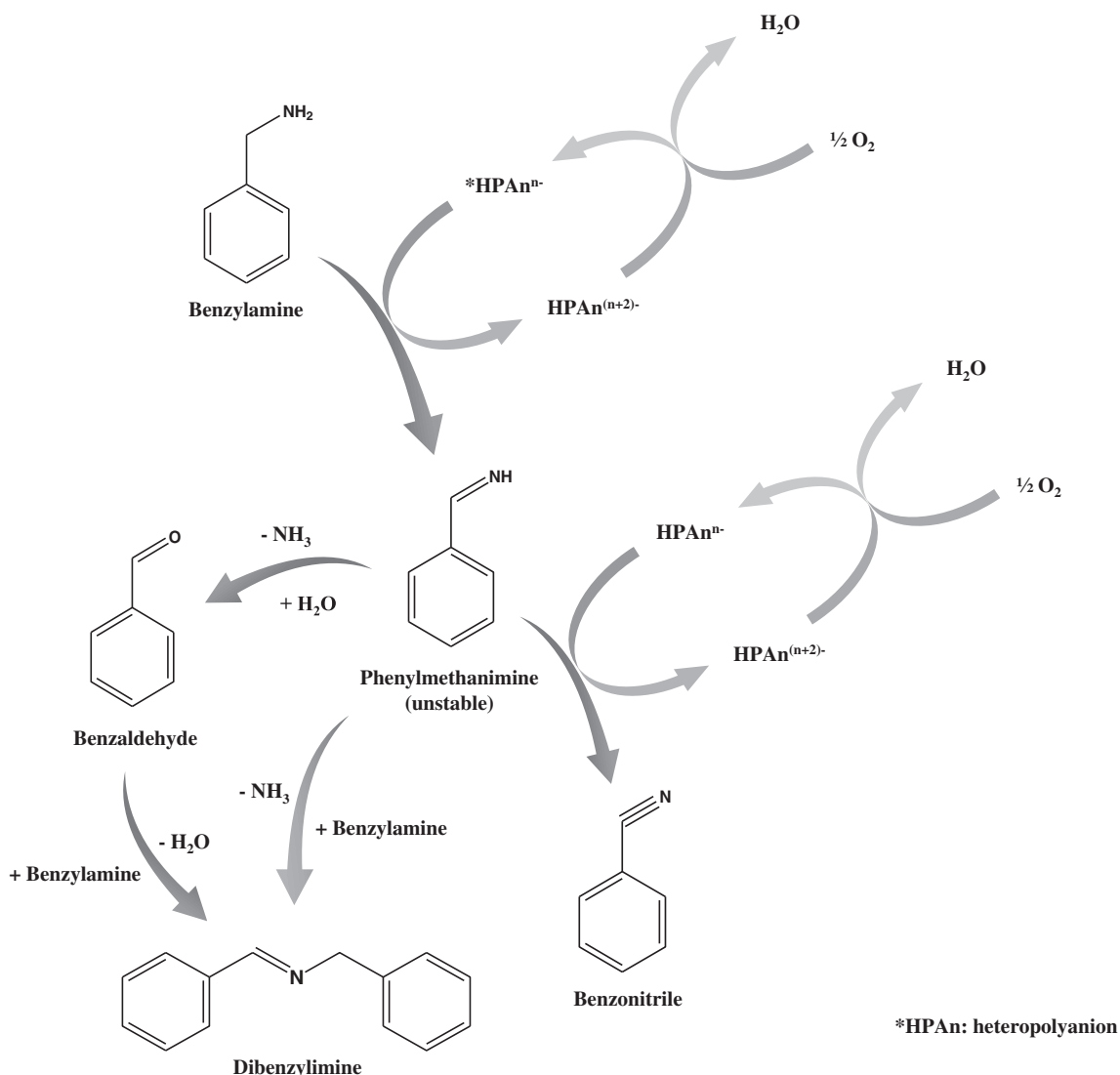


Fig. 4. Reaction pathway in the oxidative dehydrogenation of benzylamine over HPAs [16].

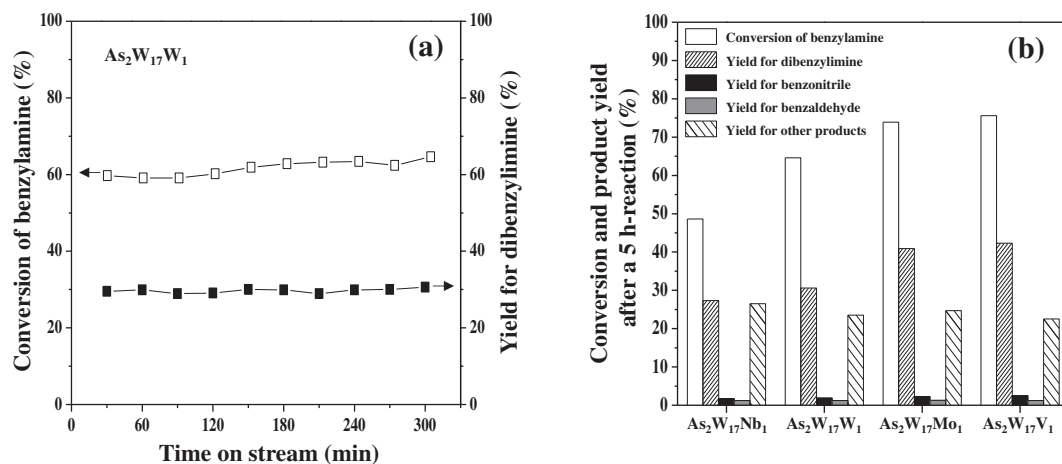


Fig. 5. (a) Catalytic performance of $As_2W_{17}W_1$ during a 5 h-reaction and (b) conversion of benzylamine and product yield after a 5 h-reaction.

observed due to the loss of water of crystallization, characteristic bands of used catalyst corresponding to $W = O_t$, $As-O$, and $W-O-W$ were maintained as observed for fresh catalyst. This result suggests that Wells–Dawson tungstoarsenate was thermally stable during the reaction at 300 °C. The other catalysts also showed similar results in the DRIFT measurements.

Fig. 7 shows the first electron reduction potential and UV–visible absorption edge energy plotted as a function of yield for dibenzylimine after a 5 h-reaction. Yield for dibenzylimine increased with increasing first electron reduction potential and with decreasing UV–visible absorption edge energy. Among the catalysts, $As_2W_{17}V_1$ (which was easier to be reduced than the other catalysts) showed the highest yield for dibenzylimine. Previous researches [4,5] have suggested that hydrogen and electron of reactant are transferred to reducible metal center and the rate-determining step involves the reduction of HPAs by hydrogen and electron in the oxidative dehydrogenation reactions. Therefore, it is inferred that the substituted vanadium center provided efficient active site for oxidative dehydrogenation by contributing to the density of accessible electronic states (unoccupied orbitals). We have demonstrated that reducibility of mono-transition metal-substituted tungstoarsenates plays an important role in determining the catalytic activity in the oxidative dehydrogenation of benzylamine.

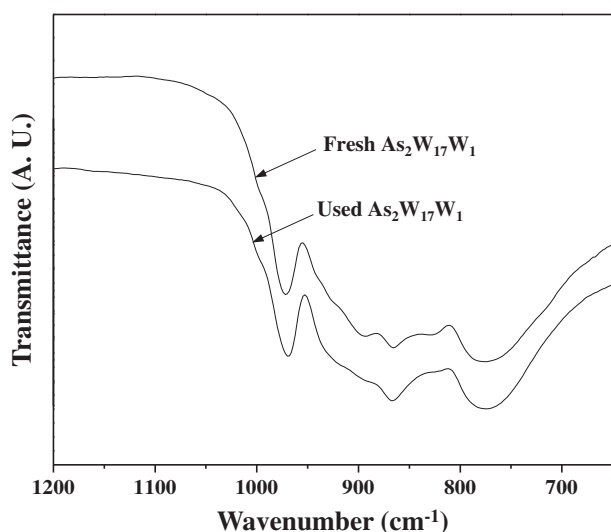


Fig. 6. DRIFT spectra of fresh and used $As_2W_{17}W_1$ catalysts.

4. Conclusions

A series of mono-transition metal-substituted tungstoarsenates were prepared and their redox behaviors were investigated by electrochemical analysis and UV–visible spectroscopy measurement. For molybdenum- and vanadium-substituted tungstoarsenates, they exhibited an additional molybdenum- and vanadium-centered redox couples at higher potential region. However, niobium-substituted tungstoarsenate showed a negatively-shifted redox couple compared to non-substituted one ($As_2W_{17}W_1$). Among the catalysts, vanadium center was more effective to enhance the reducibility of tungstoarsenate framework than any other metal centers. The results of UV–visible spectroscopy measurements revealed that energy state of the unoccupied orbitals, which depended on the nature of substituted transition metal, was closely related to redox behaviors of heteropolyanions. In the gas-phase oxidative dehydrogenation of benzylamine, yield for dibenzylimine (oxidation product) increased with increasing first electron reduction potential and with decreasing UV–visible absorption edge energy. It was successfully demonstrated that first electron reduction potential and UV–visible absorption edge energy could be utilized as alternative parameters to estimate the catalytic activity of mono-transition metal-substituted tungstoarsenates in the oxidative dehydrogenation of benzylamine.

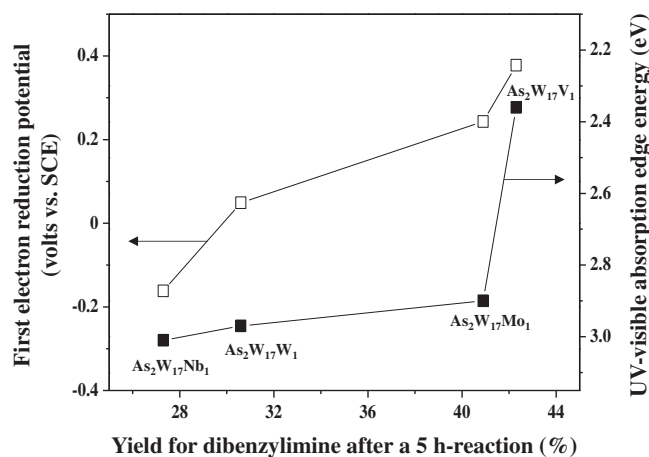


Fig. 7. First electron reduction potential and UV–visible absorption edge energy plotted as a function of yield for dibenzylimine after a 5 h-reaction.

Acknowledgments

This work was supported by the Mid-career Researcher Program of National Research Foundation (NRF) grant funded by the Korea government (MEST) (No. 2012-R1A2A4A01001146).

References

- [1] L.E. Briand, G.T. Baronetti, H.J. Thomas, The state of the art on Wells–Dawson heteropoly-compounds: a review of their properties and applications, *Appl. Catal. A Gen.* 256 (2003) 37–50.
- [2] E. Arendt, S. Zehri, P. Eloy, E.M. Gaigneaux, Supporting the Dawson $(\text{NH}_4)_6\text{P}_2\text{Mo}_{18}\text{O}_{62}$ heteropoly compound: controlling its molecular behaviour to enhance its catalytic activity in the propene oxidation, *Eur. J. Inorg. Chem.* (2012) 2792–2801.
- [3] E. Arendt, S. Ghislain, E.M. Gaigneaux, Operando investigation of the catalytic behaviour of Wells–Dawson heteropoly compounds in the oxidation of propene, *Catal. Today* 155 (2010) 227–240.
- [4] N. Mizuno, J.-S. Min, A. Taguchi, Preparation and characterization of $\text{Cs}_{2.8}\text{H}_{1.2}\text{PMo}_{11}\text{Fe}(\text{H}_2\text{O})_{39}\cdot 6\text{H}_2\text{O}$ and investigation of effects of iron-substitution on heterogeneous oxidative dehydrogenation of 2-propanol, *Chem. Mater.* 16 (2004) 2819–2825.
- [5] R.S. Weber, Molecular orbital study of C–H bond breaking during the oxidative dehydrogenation of methanol catalyzed by metal oxide surfaces, *J. Phys. Chem.* 98 (1994) 2999–3005.
- [6] J.H. Choi, T.H. Kang, Y. Bang, J.H. Song, I.K. Song, Electrochemical and UV–visible spectroscopy studies of $\text{K}_6\text{As}_2\text{W}_{18-x}\text{Mo}_x\text{O}_{62}$ ($x = 0-3$) Wells–Dawson heteropolyacid catalysts for oxidative dehydrogenation of benzyl alcohol, *Catal. Commun.* 55 (2014) 29–33.
- [7] R. Contant, R. Thouvenot, Hétéropolyanions de type Dawson. 2. Synthèses de polyoxotungstoarsénates lacunaires dérivant de l'octadécatingstodiasénate. Étude structurale par RMN du tungstène-183 des octadéca(molybdotungstovanado)diarsénates apparentés, *Can. J. Chem.* 69 (1991) 1498–1506.
- [8] P. Kubelka, F. Munk, Ein Beitrag zur Optik der farbanstriche, *Z. Tech. Phys.* 12 (1931) 593–601.
- [9] L. Adamczyk, K. Miecznikowski, Solid-state electrochemical behavior of Keggin-type borotungstic acid single crystal, *J. Solid State Electrochem.* 17 (2013) 1167–1173.
- [10] B. Keita, I.-M. Mbomekalle, L. Nadjjo, P. Oliveira, A. Ranjbari, R. Contant, Vanadium-substituted Dawson-type polyoxometalates as versatile electrocatalysts, *C. R. Chim.* 8 (2005) 1057–1066.
- [11] B. Keita, Y. Jean, B. Levy, L. Nadjjo, R. Contant, Toward a qualitative understanding of the initial electron transfer site in Dawson-type heteropolyanions, *New J. Chem.* 26 (2002) 1314–1319.
- [12] P. Villabrille, G. Romanelli, L. Gassa, P. Vázquez, C. Cáceres, Synthesis and characterization of Fe- and Cu-doped molybdovanadophosphoric acids and their application in catalytic oxidation, *Appl. Catal. A Gen.* 324 (2007) 69–76.
- [13] X. López, C. Bo, J.M. Poblet, Electronic properties of polyoxometalates: electron and proton affinity of mixed-addenda Keggin and Wells–Dawson anions, *J. Am. Chem. Soc.* 124 (2002) 12574–12582.
- [14] D.G. Barton, M. Shtein, R.D. Wilson, S.L. Soled, E. Iglesia, Structure and electronic properties of solid acids based on tungsten oxide nanostructures, *J. Phys. Chem. B* 103 (1999) 630–640.
- [15] X. López, C. Bo, J.M. Poblet, Relative stability in α - and β -Wells–Dawson heteropolyanions: a DFT study of $[\text{P}_2\text{M}_{18}\text{O}_{62}]^{n-}$ ($\text{M} = \text{W}$ and Mo) and $[\text{P}_2\text{W}_{15}\text{V}_3\text{O}_{62}]^{n-}$, *Inorg. Chem.* 42 (2003) 2634–2638.
- [16] K.T.V. Rao, B. Haribabu, P.S.S. Prasad, N. Lingaiah, Vapor-phase selective aerobic oxidation of benzylamine to dibenzylimine over silica-supported vanadium-substituted tungstophosphoric acid catalyst, *Green Chem.* 15 (2013) 837–846.